

Physicochemical Properties and Solubility of Alkyl-(2-hydroxyethyl)-dimethylammonium Bromide[†]

Urszula Domańska* and Rafał Bogel-Lukasik

Physical Chemistry Division, Faculty of Chemistry, Warsaw University of Technology,
Noakowskiego 3, 00-664 Warsaw, Poland

Received: January 12, 2005; In Final Form: March 30, 2005

Quaternary ammonium salts, which are precursors of ionic liquids, have been prepared from *N,N*-dimethylethanolamine as a substrate. The paper includes specific basic characterization of synthesized compounds via the following procedures: nuclear magnetic resonance (NMR) and Fourier transform infrared (FTIR) spectra, water content, mass spectroscopy (MS) spectra, temperatures of decompositions, basic thermodynamic properties of pure ionic liquids (the melting point, enthalpy of fusion, enthalpy of solid–solid phase transition, glass transition), and the difference in the solute heat capacity between the liquid and solid at the melting temperature determined by differential scanning calorimetry (DSC). The (solid + liquid) phase equilibria of binary mixtures containing (quaternary ammonium salt + water, or + 1-octanol) has been measured by a dynamic method over wide range of temperatures, from 230 K to 560 K. These data were correlated by means of the UNIQUAC ASM and modified nonrandom two-liquid NRTL1 equations utilizing parameters derived from the (solid + liquid) equilibrium. The partition coefficient of ionic liquid in the 1-octanol/water binary system has been calculated from the solubility results. Experimental partition coefficients ($\log P$) were negative at three temperatures.

Introduction

Ionic liquids (ILs) have attracted increasing interest recently, particularly in the area of electrochemistry, as novel solvents for chemical reactions and separations.^{1–7} Until now, we have focused on the determination of phase equilibria, (solid + liquid) phase equilibria (SLE), and (liquid + liquid) phase equilibria (LLE) of ionic liquids, based on the imidazolium cation with popular organic solvents.^{8–11} The main disadvantage of imidazolium-based ionic liquids is their relatively high cost for bulk applications, while very well-known quaternary ammonium salts seem to be much less expensive. The precursors of ionic liquids presented in this paper are tetraalkylammonium bromides with a hydroxyl group as a side chain. Quaternary ammonium compounds of natural origin, e.g., *Cinchona*-derived ammonium salts,^{12–15} have also started to be used as a phase-transition (PT) catalyst. Another very popular compound that belongs to the ammonium salts group is choline chloride (also known as vitamin B₄). It is an essential component for ensuring the proper functioning of the nervous system, and it is used widely as a feed additive for livestock.¹⁶ In addition, complexes between alkyl-(2-hydroxyethyl)-dimethylammonium salts and inorganic salts can be used in the electrodeposition of thick, adherent, crack-free films.¹⁷ That type of salt can be used as an effective media for some Diels–Alder reactions.¹⁸ That is why the full thermodynamics description of that type of salt is very important and necessary.

The most of ammonium compounds have melting points of <580 K [i.e. (2-hydroxyethyl)-trimethylammonium bromide, $T_{\text{fus}} = 573$ K].¹⁹ Many literature results suggest that both lower

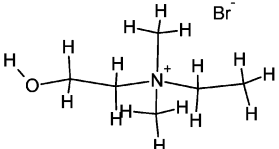
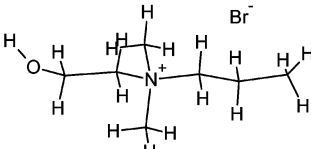
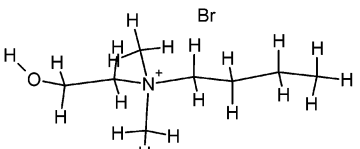
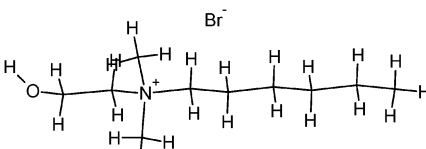
symmetry and the presence of a functional group reduce the melting or decomposition points of ammonium salts formed, although the exact role of the functional substituent is not yet clear.^{19,20} In all cases presented here, salts are solid and hygroscopic but moisture-stable, so they can be easily prepared and stored without a need for special equipment. More-complex substances with functional groups (here, a hydroxyl group) are capable of having additional interactions with polar solvents. Given their structure and diversity of functionality, they are capable of most types of interactions (i.e., dispersive, π – π , n – π , hydrogen bonding, dipolar, ionic/charge–charge, van der Waals forces). In every solution, there can be several different (in terms of type and strength) and often simultaneous solute–solvent interactions.^{20–30} The various parameters are essentially weighted averages of possible solute–solvent interactions. As the most important interaction in systems with ionic liquids the van der Waals force, hydrogen bondings,^{21–23} complexes between CO₂ and anions of ionic liquid, and Columbic interactions was described.^{7,24–26} Kazarian et al. for systems of ionic liquids with supercritical fluids (SCFs) or complexes with CO₂ count as the most important forces.^{27,28} Similar idea was presented by Baker and co-workers.²⁹ Cammarata et al. explained some relations of ILs in systems with water.³⁰ Because of interaction between two anions and one molecule of water, complex anion···HOH···anion is formed. Another important cause are possibilities to form complexes between water and cation. However, the number of molecules of water combine with ionic liquids is strongly dependent on the spherical structure of cation and anion. When the anion, or cation, are planar, or almost planar, the number of water molecules possible to form hydrogen bond with anion, or cation increases.

The ILs miscibility or immiscibility with water or 1-octanol is dependent on the substituents on the cation or dependent on the type of anion. The complete understanding of the phase

* To whom correspondence should be addressed. E-mail: ula@ch.pw.edu.pl.

[†] Presented at the 18th IUPAC Conference on Chemical Thermodynamics, Beijing, China, 17–21.08.2004.

TABLE 1: Investigated Compounds: Structure, Names and Abbreviations of Names

structure	name	abbreviation
	Ethyl-(2-hydroxyethyl)- dimethylammonium bromide	C ₂ Br
	(2-Hydroxyethyl)-dimethyl- propylammonium bromide	C ₃ Br
	Butyl-(2-hydroxyethyl)- dimethylammonium bromide	C ₄ Br
	Hexyl-(2-hydroxyethyl)- dimethylammonium bromide	C ₆ Br

behavior of ILs with water is an important issue. The problem of partitioning benzene and its substituents between IL [bmim]-[PF₆]/water and 1-octanol/water with regard to a possible use for the LLE process was presented earlier.³¹ The 1-octanol/water partition coefficients for 1,3-dialkyl-imidazolium salts, were under our investigations previously.⁸

This work includes synthesis, physicochemical properties, and the phase equilibria measurements of four quaternary ammonium salts such as: ethyl-(2-hydroxyethyl)-dimethylammonium bromide (C₂Br), (2-hydroxyethyl)-dimethyl-propylammonium bromide (C₃Br), butyl-(2-hydroxyethyl)-dimethylammonium bromide (C₄Br), and hexyl-(2-hydroxyethyl)-dimethylammonium bromide (C₆Br). This paper is the first part of our wide range of investigations into quaternary ammonium salts, also with other type of anions, such as BF₄⁻, PF₆⁻, N(CN)₂⁻, and NTf₂⁻. Usually, salts that are based on halide anions have higher melting points than salts with larger, more-complex anions.

Notably, some alkyl-(2-hydroxyethyl)-dimethylammonium tetrafluoroborates, hexafluorophosphates, and bis(trifluoromethylsulfonyl)imides are liquid at room temperature.

Experimental Procedures and Results

Preparation and Purification of Compounds. Investigated compounds were prepared using a different method, contrary to the previously published procedure.³² The *N,N*-dimethylethanolamine (Sigma–Aldrich, CAS No. 108-01-0) and an appropriate haloalkane, such as ethyl bromide (Sigma–Aldrich, CAS No. 74-96-4), propyl bromide (Sigma–Aldrich, CAS No. 106-94-5), butyl bromide (Sigma–Aldrich, CAS No. 109-65-9), or hexyl bromide (Sigma–Aldrich, CAS No. 111-25-1) were placed into a round-bottom flask. The reagents were mixed in 10% excess of haloalkane. The intermediates were heated at 80°C for 30 min and stirred under reflux to form the reaction mixture. The mixture then was cooled and the obtained solid product was dissolved in a mixture of 1-propanol (Sigma–Aldrich, CAS No. 71-23-8) and methanol (Sigma–Aldrich, CAS

No. 67-56-1) at ratio of 1:3. Subsequently, the mixture was heated at 80 °C for 30 min under reflux. Later, the mixture was cooled and cyclohexane (Sigma–Aldrich, CAS No. 110-82-7) in very small portions was added into the mixture to form the solid powder. The solid phase was filtered through the S4 filter, and that phase was collected. Next, to the liquid phase, a portion of cyclohexane was added to the completely give off the product. All salts were recrystallized from a mixture of 1-propanol and methanol and then rigorously dried under vacuum for 48 h prior to use. We believe that the solvents and unreacted reagents (even we know that amine is not volatile enough) were removed under vacuum from the white solid, which was obtained with a yield of >88%. The compounds were characterized using Fourier transform infrared (FTIR) spectroscopy, nuclear magnetic resonance (NMR), mass spectroscopy (MS), and elemental analysis. The brief characterization of obtained compounds is presented in Table 1.

1-Octanol was produced by Sigma–Aldrich Chemie GmbH, Steinheim, Germany, and was fractionally distilled to a purity of >99.8 mass %. The solvent was stored over freshly activated molecular sieves of type 4A (Union Carbide). Twice distilled and degassed water was used for the solubility measurements.

Nuclear Magnetic Resonance (NMR). ¹H NMR and ¹³C NMR spectra in D₂O, CDCl₃, or CD₃OD solutions were recorded on a Varian model Gemini 2000 spectrometer. A description of the spectra is presented as GRS 1 in the Supporting Information.

Fourier Transform Infrared Spectroscopy (FTIR). The FTIR spectra were recorded as KBr pellets (for solid), or with crystal ZnSe (for solutions) inside a nitrogen atmosphere glovebox, using Perkin–Elmer System 2000 equipment. Spectra were recorded with a resolution of 2 cm⁻¹. A description of the spectra is presented as GRS 2 in the Supporting Information.

Mass Spectroscopy. MS spectra were recorded on a Hewlett–Packard HP 5980 Series II gas chromatograph that was connected to a Hewlett–Packard model HP 5971 mass detector.

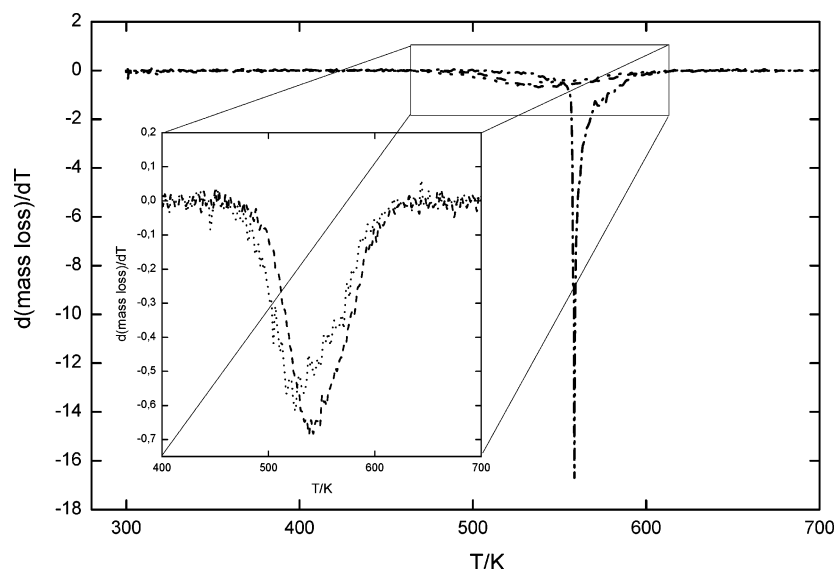


Figure 1. Decomposition ($d(\text{mass loss})/dT$) curves of the thermal degradation of $C_n\text{Br}$ salts: (— · —) $C_2\text{Br}$, (---) $C_3\text{Br}$, and (···) $C_4\text{Br}$.

The solutions were prepared by dissolving compounds in methanol. Helium was used as the carrier gas in the column with a flow rate of 1 mL/min. The separation was conducted using a low-polarity model HP-35 column (Hewlett–Packard). A description of the spectra is presented as GRS 3 in the Supporting Information.

Elemental Analysis. Elemental analysis was performed using a Perkin–Elmer Series II Model 2400 CHNS/O analyzer. Elementary analysis results are presented in Table 1S in the Supporting Information.

Water Content. Water content was analyzed using the Karl Fischer titration technique (method TitroLine KF). Samples of all compounds were dissolved in methanol and titrated with a step of 2.5 μL . The results are presented in Table 2S in the Supporting Information.

Decomposition of Compounds. Simultaneous thermogravimetry/differential thermal analysis (TG/DTA) experiments were performed using a MOM Derivatograph–PC (Hungary). Generally, runs were performed using matched labyrinth platinum crucibles with Al_2O_3 in the reference pan. The crucible design hampered the migration of volatile decomposition products, reducing the rate of gas evolution and, in turn, increasing contact time of the reactants. All TG/DTA curves were obtained at a heating rate of 5 K/min with a dynamic nitrogen atmosphere (flow rate of 20 $\text{dm}^3 \text{h}^{-1}$). The decomposition temperatures and mass-loss percentages are presented in Table 3S in the Supporting Information. Figures 1 and 2 present comparisons of decomposition and mass-loss percentage, respectively, for every salt.

Differential Scanning Microcalorimetry (DSC). The melting point, the enthalpy of fusion, and the enthalpy of the solid–solid phase transition of quaternary ammonium salts were measured via differential scanning calorimetry (DSC), using a differential scanning microcalorimeter at a scan rate of 5 K/min with a power sensitivity of 16 mJ/s and with the recorder sensitivity of 5 mV. Each time the instrument (Perkin–Elmer Pyris 1) was used, it was calibrated with the 99.9999 mol % purity indium sample. The calorimetric accuracy was $\pm 1\%$, and the calorimetric precision was $\pm 0.5\%$. The thermophysical properties are shown in Table 2.

The heat capacity per unit volume of melting was measured under atmospheric pressure using a Setaram model TG-DSC 111 differential scanning calorimeter, on the basis of the Calvet's

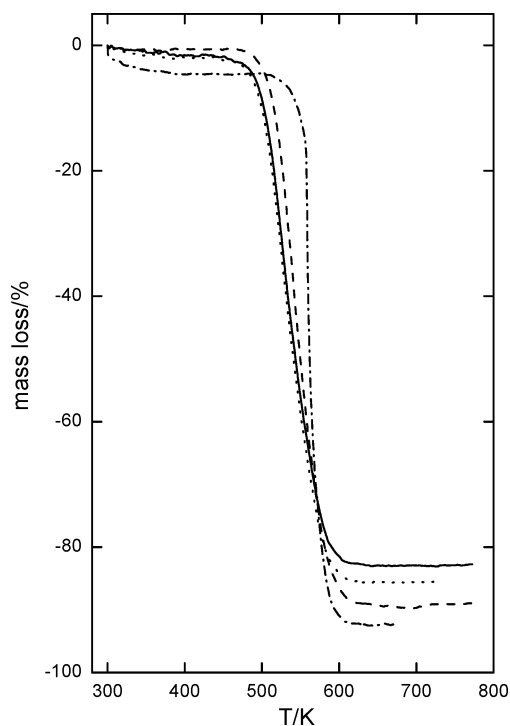


Figure 2. Thermogravimetric analysis (TGA) curves of the thermal degradation of $C_n\text{Br}$ salts: (— · —) $C_2\text{Br}$, (---) $C_3\text{Br}$, (···) $C_4\text{Br}$, and (—) $C_6\text{Br}$.

principle. The heat-capacity measurements were made during the heating process. The range is dependent on the melting point of the investigated compounds. The measurements were performed via the “step with reference” method, using a scanning rate of 0.5 K/min over a wide range of temperature. Al_2O_3 was used as a reference sample of known heat capacity. The heat capacity in the solid and liquid phases are presented in Table 4S in the Supporting Information.

(Solid + Liquid) Phase Equilibria Apparatus and Measurements. Solid solubilities have been determined using a dynamic (synthetic) method that has been described previously.³³ The compound was provided under the nitrogen in the dry box. Mixtures of the solute and solvent were prepared by weighing the pure components to a precision within 1×10^{-4} g. The sample of solute and solvent was heated very slowly (at < 2

TABLE 2: Thermophysical Constants of Pure C_n Br Salts, Determined from Differential Scanning Calorimetry (DSC) Data^a

compound	$T_{\text{fus},1}$ (K)	$\Delta_{\text{fus}}H_1$ (kJ/mol)	$T_{\text{tr},1}$ (K)	$\Delta_{\text{tr}}H_1$ (kJ/mol)	$\Delta_{\text{fus}}C_{p1}$ (J mol ⁻¹ K ⁻¹)
C ₂ Br	541.45	25.56	347.14; 216.26 (g) ^b	3.66	
C ₃ Br	372.59	4.12	347.44; 339.16; 319.93; 166.35 (g) ^c	0.63; 3.07; 4.72	-75.3
C ₄ Br	359.34	13.21	187.31 (g) ^d		-97.9
C ₆ Br	355.34	3.78	184.66 (g) ^e		-5.8

^a The symbol (g) denotes glass transition. ^b ΔC_p at the glass transition is equal to 1.5 J mol⁻¹ K⁻¹. ^c ΔC_p at the glass transition is equal to 12.4 J mol⁻¹ K⁻¹. ^d ΔC_p at the glass transition is equal to 30.9 J mol⁻¹ K⁻¹. ^e ΔC_p at the glass transition is equal to 59.7 J mol⁻¹ K⁻¹.

K/h near the equilibrium temperature) with continuous stirring inside a Pyrex glass cell and placed in a thermostat. The crystal disappearance temperatures, detected visually, were measured with a calibrated Gallenkamp Autotherm II thermometer that was totally immersed in the thermostating liquid. The measurements were conducted over a wide range of solute mole fractions (from 0 to 1). The uncertainty of temperature measurements was ± 0.01 K, and that of the mole fraction did not exceed ± 0.0005 .

Results. The quick and trivial method of synthesis allowed us to receive quaternary ammonium salts with unique features. *N,N*-Dimethylethanolamine and haloalkane were used at a ratio that permitted the formation of a final product free from all amounts of amine, which is difficult to remove via vacuum. The method that was used allowed us to obtain purer compounds with high yield, according to the settlements of Montreal Protocol and "green chemistry". The NMR technique of two nuclei, such as ¹H and ¹³C, present the pure salts without unexpected signals, i.e., from unremoved solvents or unreacted intermediates. FTIR analysis was used to describe the obtained compounds and to determine the purity of the synthesized salts. Analyzing FTIR spectra, it can be noticed that the dissolved salts exhibit the ability to form a hydrogen bond between the -OH group from quaternary ammonium salts and the -H species from the solvent (i.e., from water or an alcohol) and also exhibit the ability to form a hydrogen bond between two solute molecules. As a proof of that, the signal of the associated -OH group is more intensive and wider, compared to that obtained for KBr disk, and the signal becomes more intensive and wider when the amount of water increases in the investigated mixture. Similar results were discussed by Cammarata and co-workers.³⁰ Through comparison of the infrared (IR) signals for other groups in the solid and liquid phase, it can be concluded that only the -OH group from bromide could form a hydrogen bond with the solvent.

MS spectra indicate that the strongest signals belong to CH₃-NCH₃ and CH₂CH₂N(CH₃)₂ groups for ethyl-(2-hydroxyethyl)-dimethylammonium bromide. The analysis of other salts leads us to make the statement that, when the alkyl chain in alkyl-(2-hydroxyethyl)-dimethylammonium bromide is longer, the strongest signal is observed for the CH₂CH₂NCH₃ group.

Elemental analysis results verify the high purity of obtained compounds, because they are similar to calculated values. The difference between the found and calculated values is the highest for the hydrogen of butyl-(2-hydroxyethyl)-dimethylammonium bromide and is equal to 0.33%. The smallest difference is for hydrogen for ethyl-(2-hydroxyethyl)-dimethylammonium bromide, and it is equal to 0.00%.

The salts obtained demonstrate high decomposition temperatures. For investigated components, the temperature of decomposition is strongly dependent on the alkyl chain length. The decomposition temperature is the highest for the shortest alkyl chain in the cation and is equal to 559.35 K for C₂Br. For the longer alkyl chain, the decomposition temperature decreases to 525.27 K for C₄Br (see Figure 1). Compounds have been

decomposed in one step. The mass-loss percentage of ionic liquids decreases as the alkyl chain length increases. The highest value was obtained for C₂Br (92.25%), and the lowest was observed for C₆Br (does not exceed 82.8%). Results are shown in Figure 2.

The thermograph of ethyl-(2-hydroxyethyl)-dimethylammonium bromide shows that this salt exhibits a very high melting temperature, equal to 541.45 K with a heat of fusion equal to 25.56 kJ/mol. On the other hand, the solid-solid phase transition of C₂Br, accompanied by the heat effect equal to 3.658 kJ/mol at 347.14 K, was observed. The obtained melting point of C₂-Br is lower than that presented earlier (558.15 K).¹⁹

The DSC diagram for C₃Br presents the melting point at 372.59 K, with a heat of fusion of $\Delta_{\text{fus}}H = 4.12$ kJ/mol and the visible three solid-solid phase transitions at 347.44, 339.16, and 319.93 K with corresponding heats of phase transition equal to 0.63, 3.07, and 4.72 kJ/mol. The enthalpies of the three solid-solid phase transitions diminish the enthalpy of melting of C₃-Br, because usually these effects (the enthalpies of solid-solid phase transitions) are shown as a sum with the enthalpy of melting. This phenomenon is not observed for two other investigated salts: C₄Br and C₆Br. Also, the glass-transition temperature is ~ 20 K lower than that for C₄Br and C₆Br. In our work, similar results were obtained by different DSC calorimeters, i.e., during the heat-capacity measurements.

To our knowledge, this is the first time the difference in solute heat capacity between the liquid and solid at the melting temperature has been determined by the DSC analysis of ILs or their precursors. The heat capacity of the investigated compounds was measured at the liquid and solid state, and the difference in the melting temperatures was calculated. The results of the heat capacity changing as a function of temperature are listed in Table 4S in the Supporting Information. The heat capacity of ethyl-(2-hydroxyethyl)-dimethylammonium bromide was not determined, because the temperature range of liquid phase after melting and before decomposition was too narrow. The difference in the heat capacity of solute ($\Delta_{\text{fus}}C_{p1}$) of the investigated compounds is presented in Table 4S. Figure 3 shows the change in the molar heat capacity at the melting temperature of C₃Br as an example. The sixth-order polynomials presented in the graph describe the parameter C_p as a function of temperature for the solid and liquid phase of pure salt. Experimental points presented here are only a part of wider examinations.

Solubilities of C_n Br in 1-octanol and water are shown in Tables 5S and 6S in the Supporting Information. These tables include the direct experimental results of the SLE, using temperature (T_1) versus the mole fraction of the solute (x_1).

The SLE experimental phase diagrams investigated in this work are not easy to interpret, inherently because solutes are very complicated and involve highly interacting molecules, especially in water and alcohol. The solubility of C_n Br in 1-octanol increases when the alkyl chain of cation increases over almost the entire concentration range. These results are presented in Figure 4. In water, the solubility of C₂Br is much

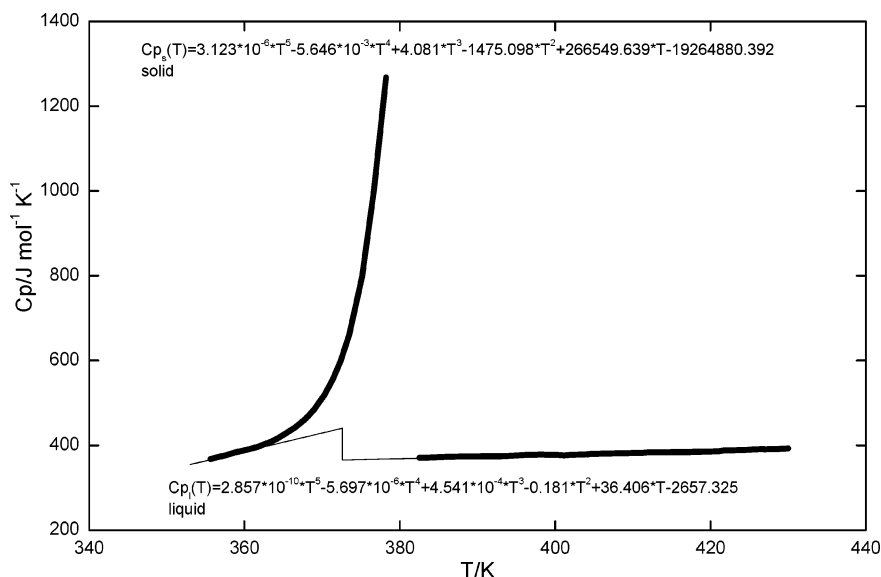


Figure 3. Change in molar heat capacity at the melting temperature ($\Delta_{\text{fus}}C_p$) of C_3Br . Equations in the figure present the ΔC_p as a function of temperature in the solid (thick line) and liquid (thin line) phases; the thin lines are calculated by sixth-order polynomials for both phases.

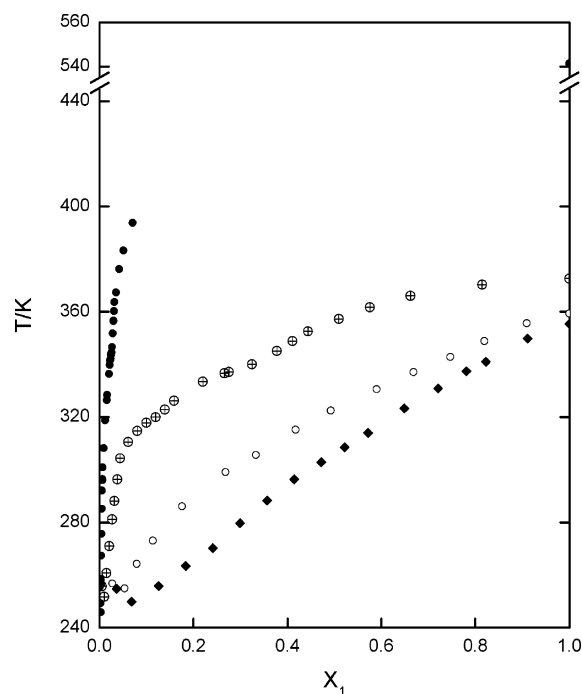


Figure 4. (Solid + liquid) phase equilibria of $(\text{C}_n\text{Br} + 1\text{-octanol})$: (●) C_2Br , (⊕) C_3Br , (○) C_4Br , and (◆) C_6Br . Data points represent the experimental results.

smaller than the other three salts and the best solubility was also observed for C_6Br (see Figure 5). The results are mainly dependent on the melting temperature and the enthalpy of melting of the solute. It can be stated that a short alkane substituent at the ammonium cation causes the highest melting temperature and the worst solubility of this salt is observed in 1-octanol and water. Analysis of the temperature of fusion (T_{fus}) and decomposition shows the highest temperature of fusion ($T_{\text{fus}} = 541.45 \text{ K}$) and decomposition (559.35 K) for C_2Br , which is undoubtedly the result of the intramolecular hydrogen bonding caused by the hydroxyl side group on the one alkyl chain. For a short ethyl substituent, it is also the result of the high packing effect in the crystal structure of the salt. For a longer alkyl chain, as it is in C_6Br , the steric effects are the reasons for lower intramolecular interactions (lower hydrogen bonding), lower

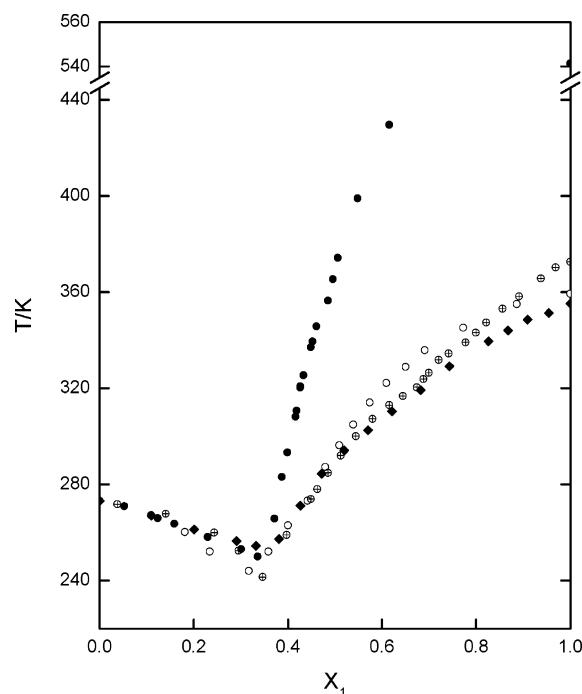


Figure 5. (Solid + liquid) phase equilibria of $(\text{C}_n\text{Br} + \text{water})$: (●) C_2Br , (⊕) C_3Br , (○) C_4Br , and (◆) C_6Br . Data points represent the experimental results.

melting temperature (355.34 K), much lower enthalpy of fusion (25.56 kJ/mol for C_2Br , versus 3.78 kJ/mol for C_6Br), and an $\sim 35 \text{ K}$ lower decomposition temperature. The solubility of alkyl-(2-hydroxyethyl)-dimethylammonium bromides in polar solvents as water and alcohol increases as the alkyl chain length of the substituent at the N atom increases, which is a result of greater intermolecular hydrogen bonding between the salt and the solvent. Similar effects were observed in the LLE measurements. By extending the alkyl chain from an ethyl group to an octyl group (i.e., 1-alkyl-3-methylimidazolium hexafluorophosphate ionic liquids with 1-butanol and other ILs in different alcohols), the upper critical solution temperature decreases and the ionic liquid–alcohol mutual solubilities increase.²¹ The enhancement in solubility with increased alkyl chain length was explained by the increased ability of longer alkyl chain on the

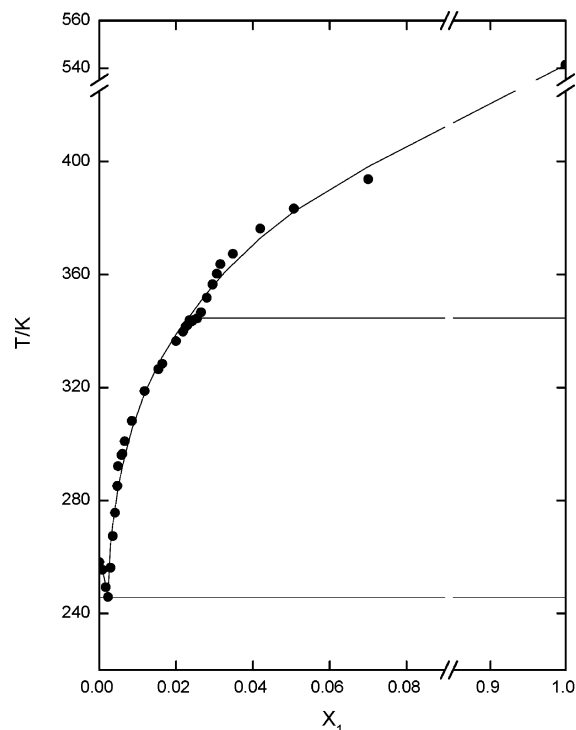


Figure 6. (Solid + liquid) phase equilibria of (C_2Br + 1-octanol). Data points represent the experimental results; solid lines are calculated by the UNIQUAC ASM model.

cation to interact with the alkyl portion of the alcohol via van der Waals interaction.²¹ Opposite effects were observed for imidazolium ionic liquids in water, because there is no alkyl chain in water with which the van der Waals interaction may occur. Our new results are opposite to those presented earlier for 1-alkyl-3-methylimidazolium chlorides, but for much-longer alkane chains (C_4 vs C_{12}) in 1-octanol and water.⁸

The liquidus curve of C_2Br has shown one characteristic inflection of the solid–solid phase transition [see binary system (C_2Br + 1-octanol) in Figure 6], whereas the liquidus curves of C_3Br have shown three solid–solid phase transitions in both solvents [see binary system (C_3Br + water) in Figure 7].

Because of the complete phase diagrams of investigated compounds in 1-octanol and in water, the eutectic points were determined graphically. Table 7S in the Supporting Information lists the temperatures and compositions of the eutectic points for the investigated mixtures. Complete SLE diagrams for the rest of mixtures are presented in Figures 1S–6S in the Supporting Information. The observed eutectic points for the mixtures of (C_nBr + 1-octanol), in comparison to this current mixture (C_nBr + water), are shifted toward much lower salt mole fractions.

Correlation of (Solid + Liquid) Equilibrium. The solubility of a solid 1 in a liquid may be expressed in a very general manner by eq 1:

$$-\ln x_1 = \frac{\Delta_{\text{fus}}H_1}{R} \left(\frac{1}{T_1} - \frac{1}{T_{\text{fus},1}} \right) + \frac{\Delta_{\text{tr}}H_1}{R} \left(\frac{1}{T_1} - \frac{1}{T_{\text{tr},1}} \right) - \frac{\Delta_{\text{fus}}C_{p1}}{R} \left[\ln \left(\frac{T_1}{T_{\text{fus},1}} \right) + \frac{T_{\text{fus},1}}{T_1} - 1 \right] + \ln \gamma_1 \quad (1)$$

where x_1 is the mole fraction, γ_1 the activity coefficient, $\Delta_{\text{fus}}H_1$ the enthalpy of fusion, $\Delta_{\text{fus}}C_{p1}$ the difference in solute heat capacity between the liquid and solid at the melting temperature, $T_{\text{fus},1}$ the melting temperature of the solute (1), and T_1 the

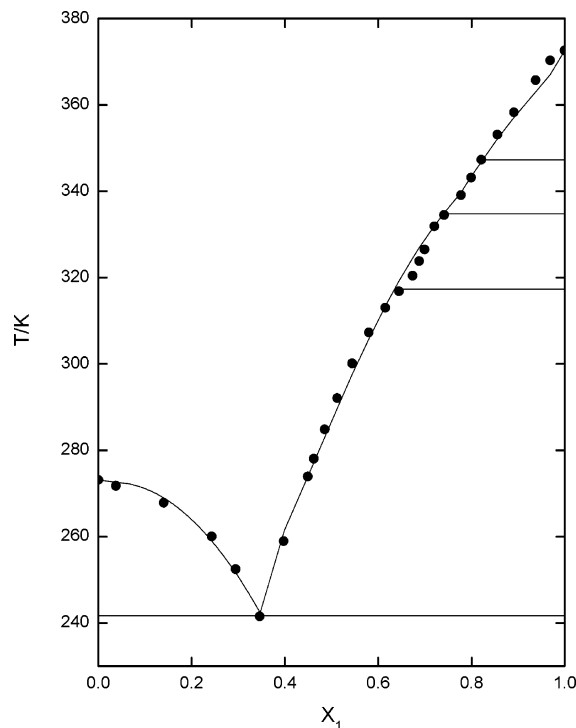


Figure 7. (Solid + liquid) phase equilibria of (C_3Br + water). Data points represent the experimental results; solid lines are calculated by the NRTL 1 model.

equilibrium temperature. The terms $\Delta_{\text{tr}}H_1$ and $T_{\text{tr},1}$ are the enthalpy of the solid–solid phase transition and the transition temperature of the solute, respectively (used for C_2Br and C_3Br). Unfortunately, the value of $\Delta_{\text{fus}}C_{p1}$ for C_2Br could not be determined and eq 1 was used in the calculations without the third term. Equation 1 may be used, assuming the simple eutectic mixtures with full miscibility in the liquid and immiscibility in the solid phases.

In this study, two methods were used to derive the solute activity coefficients γ_1 from the so-called correlation equations that describe the Gibbs free energy of mixing, (G^E): the UNIQUAC ASM theory³⁴ and NRTL1 theory.³⁵ The UNIQUAC associated-solution theory has been proposed to reproduce the (vapor + liquid), (liquid + liquid), and (solid + liquid) phase equilibria of binary (alcohol + unassociated component, or alcohol) mixtures, as well as for ternary mixtures of two alcohols with one nonpolar component. The model postulates the formation of linear multisolvated complexes from i -mers of one or two alcohols. The association equilibrium constants was assumed to be independent of the degree of association and solvation.³³ The modified form of the NRTL equation proposed by Renon was presented by Nagata and co-workers³⁵ by substituting the local surface fraction for the local mole fraction and further by including Guggenheim's combinatorial entropy for athermal mixtures whose molecules differ in size and shape. The result equations involve three adjustable parameters and are extended to multicomponent systems without adding ternary parameters.

Two adjustable parameters of the equations were found by an optimization technique using Marquardt's or Rosenbrock's maximum likelihood method of minimization:

$$\Omega = \sum_{i=1}^n [T_i^{\text{exp}} - T_i^{\text{cal}}(x_{1i}, P_1, P_2)]^2 \quad (2)$$

where Ω is the objective function, n is the number of

experimental points, and T_i^{exp} and T_i^{cal} denote, respectively, the experimental and calculated equilibrium temperature corresponding to the concentration x_{1i} . P_1 and P_2 are model parameters that result from the minimization procedure. The root-mean-square (rms) deviation of temperature was defined as follows:

$$\sigma_T = \left[\sum_{i=1}^n \frac{(T_i^{\text{exp}} - T_i^{\text{cal}})^2}{n-2} \right]^{1/2} \quad (3)$$

The parameters r_i and q_i of the UNIQUAC ASM model were calculated using following relationships:

$$r_i = 0.029281V_m \quad (4)$$

$$q_i = \frac{(Z-2)r_i}{Z} + \frac{2(1-l_i)}{Z} \quad (5)$$

where V_m is the molar volume of pure compound i at 298.15 K. The molar volumes of solute V_{m_i} (298.15), for hypothetical subcooled liquids, were calculated by the group contribution method³⁶ and were assumed to be 179.8, 195.9, 212.0, and 244.2 cm³/mol, respectively, for $n = 2, 3, 4$, and 6. The coordination number Z was assumed to be equal to 10 and the bulk factor l_i was assumed to be equal to 0 for the linear molecule. The calculations were performed using a data set of association: $K = 81.7$ and $-\Delta h_h = 21.9$ kJ/mol at 298.15 K for alcohol as a solvent,³⁷ and $K = 1036$ and $-\Delta h_h = 25.60$ kJ/mol at 323.15 K for water.³³ The temperature dependence of association constants was calculated from the van't Hoff relation, assuming that the enthalpy of hydrogen-bond formation is independent of temperature. The Kretschmer–Wiebe model of association was used. The correlation for the two used equations was presented with the development of two adjustable parameters. In this work, the value of parameter α ($\alpha = 0.1, 0.45, 0.5, 0.6$, or 0.99), which is a constant of proportionality similar to the nonrandomness constant of the NRTL 1 equation, was used in the calculations for different binary systems.

Values of model parameters obtained by fitting solubility curves together with the corresponding standard deviations are given in Table 8S in the Supporting Information. For the systems presented in this work, the description of the (solid + liquid) phase equilibrium was given by the average standard mean deviation (σ_T) which is equal to 5.84 and 2.98 K for the UNIQUAC ASM and NRTL 1 equations, respectively. Such a result is also evident that the additional term for the association of solvent only (UNIQUAC ASM) is not sufficient for the systems under study, because of the strong solute–solvent interaction. The comparison of two equations used is shown in Figure 3S in the Supporting Information, where the SLE diagram of (C₄Br + 1-octanol) is presented, together with curves calculated by the NRTL1 equation [solid line represents the rms deviation of temperature, $\sigma_T = 0.67$ K (see Table 8S in the Supporting Information)] and UNIQUAC ASM equation [dashed line represents the rms deviation of temperature, $\sigma_T = 3.94$ K (see Table 8S)].

Positive and negative deviations from ideality were observed. The differences from ideality were not significant in most of the systems. The values of the activity coefficients in the saturated solution were in the range of 0.4–15.0 (see Tables 5S and 6S in the Supporting Information). Figure 3S presents the comparison between the ideal solubility and the experimental points for C₃Br in 1-octanol. Lower-than-ideal solubility was observed.

TABLE 3: Experimental log P , 1-Octanol/Water Partition Coefficient, as a Function of Temperature for C_{*n*}Br Salts

substance	log P (288.15 K)	log P (298.15 K)	log P (308.15 K)
C ₃ Br	−0.82	−0.81	−0.79
C ₃ Br	−0.66	−0.62	−0.59
C ₄ Br	−0.44	−0.37	−0.29
C ₆ Br	−0.25	−0.19	−0.14

1-Octanol/Water Partitioning. The partition coefficient is normally used to assess the potential bioaccumulation and the distribution pattern of drugs and pollutants. As we mentioned previously, vitamin B₄ belongs to the same group, which we present here. That is why, in our opinion, salts presented in this work should be nontoxic and the values of the logarithm of partition coefficients of these salts in 1-octanol/water systems were expected to be negative. The results of solubilities in 1-octanol and water have given the basis for calculation of the partition coefficients of alkyl-(2-hydroxyethyl)-dimethylammonium bromides in the 1-octanol/water system at three temperatures.

Because of the high solubility of ionic liquids in 1-octanol and water, we have used a simple, synthetic, visual method, which has been described previously. The experimental results at temperatures of 288.15, 298.15, and 308.15 K are reported in Table 9S in the Supporting Information. It is evident that the low aqueous solubility of 1-octanol has a negligible influence on the aqueous solubility of C_{*n*}Br. On the other hand, the rather large amount of water presented in the 1-octanol phase (“solute free” $x_w^0 = 0.29$)³⁹ changes the C_{*n*}Br solubilities in the 1-octanol phase considerably, even if the simple linear dependence for binary “solute-free” solvent was assumed. Corresponding values of the C_{*n*}Br solubilities in mutually saturated solvent, as a molar concentration in water-saturated 1-octanol, (c_1^{0*}) and 1-octanol-saturated water, (c_1^{w*}), are given in Table 9S. As shown, the solute partition coefficient, which is defined as $P = c_1^{0*}/c_1^{w*}$, of C_{*n*}Br is <1. Indeed, the 1-octanol/water partition coefficient for salts used as solvents in new “green technology”, is used to evaluate the hydrophobicity of a compound, in the field of environmental science. As presented in Table 3, with an increase of the alkyl chain from 2 C atoms to 6 C atoms, the value of the logarithm of 1-octanol/water partition coefficient P increases (is less negative), which means that rather short chain substituents may be suggested as a “green substances” for new technologies. The influence of temperature is not significant: the log P value increases (is less negative) as temperature increases.

Concluding Remarks

We have presented a rapid and easy method for the synthesis of alkyl-(2-hydroxyethyl)-dimethylammonium bromides (where the alkyl portion is an ethyl, propyl, butyl, or hexyl substituent). These rather high melting compounds could be used as the precursors of new quaternary ionic liquids (ILs) or the phase-transfer (PT) catalyst, additives to new processes for large-scale electroplating, or substances that enhance the lubricate properties of the motor oils, or anticorrosive additives. Because of their large solubility in water and alcohols, which is a result of a hydroxyl group at a side chain, the possible new application can be tested as wood preservatives. In the early 1980s, quaternary ammonium chlorides or bromides (didecylidimethylammonium) were used as the first generation of wood preservatives, which were freely water-soluble, were easy to handle, and did not create environmental or health problems.⁴⁰

By extending the alkyl chain from an ethyl group to a propyl group to a butyl group to a hexyl group, the melting temperature of salt decreases. Full details about the structural features lowering the melting point of (*n*-hydroxyalkyl)-trialkylammonium bromides via the quantitative structure property relationship (QSPR) method were published earlier.¹⁹ There were descriptors indicating that increasing alkyl chain lengths will increase the melting point. However, when the asymmetry of the molecule (long alkyl chain along with two or three shorter ones) is increased and the fractional charge-weighted positive partial surface area descriptor for a long chain alkane is decreased (hydrogen less positively charged on long alkyl chain), as well as when the total negative charge of the molecule (the largest negative partial charge is located on the oxygen of the hydroxyl group) is increased (increasing the chain length), one can expect a lowering of the salt's melting point.¹⁹ Also, the total polar surface area descriptor indicates that the shorter alkyl chains (here two methyl groups) around the N atom are better.¹⁹ In conclusion, the melting temperatures of the salts under study are the results of many different factors.

The phenomenon of three solid–solid phase transitions for C₃Br and one for C₂Br ionic liquids has been observed in the temperature range of 150–600 K. The solid–solid phase transition, as a result of the changing structure of a solid phase at constant temperature and pressure, is widely used in energy storage. In our work, C₃Br was a compound with a specific crystal structure, which is easy to change by decreasing the temperature at constant pressure. This is probably the result of symmetrical substitutes on two sites of the N atom (–CH₂CH₂–CH₃ vs –CH₂CH₂OH) plus two other dimethyl substituents. The comparison of the summary melting and transition effects shows that the lowest heat effect was obtained for C₃Br (12.54 kJ/mol for C₃Br, versus 29.22 kJ/mol for C₂Br and 13.21 kJ/mol for C₄Br). This is the evidence that the structure of C₃Br may be easily changed. Unfortunately, the structures of the obtained salts were not described, because the crystallization process is very complicated and did not result in the formation of monocrystals.

Negative values of $\Delta_{\text{fus}}C_{p1}$ at the melting temperature were observed, which is not typical for organic substances. This is a result of sharp increases of heat capacity with an increase of temperature in the liquid phase, contrary to that observed in the solid phase. Such a phenomenon was observed previously for tridecane, octanhydro-anthracene, 4-methylphenanthrene, pentadecane, and hexadecane.⁴¹

The applied salts have been surprisingly soluble with 1-octanol and water. For all investigated ammonium salts, an increase in the alkyl chain length of the substituent resulted in an increase in the solubilities in water and 1-octanol. The solubility of C_{*n*}-Br in water is greater than that in 1-octanol. The difference between the solubilities of C_{*n*}-Br (where *n* = 2, 3, 4, 6) in water and 1-octanol decreases as the alkyl chain length of the cation increases. Obtained results confirm that the hydrophobicity of ILs decreases as the alkyl chain length of the cation increases. One may conclude that, when the alkyl chain increases, the A–A association of the solute decreases, the A–B interaction increases, and the solubility increases. A greater effect of the alkane chain is observed in water.

The (solid + liquid) phase diagrams have shown simple eutectic mixtures. The results of the correlation were much better with the NRTL 1 equation and the optimization was also used as an approximate description of the activity coefficients.

The logarithm of the 1-octanol/water partition coefficient is negative, as it was observed for 1,3-dialkylimidazolium chlo-

rides.⁸ In comparison to the conventional organic substances, the presented salts are much more complex solute systems that are capable of undergoing many types of interactions. In the binary mixtures of (C_{*n*}Br + 1-octanol, or water), mainly the hydrogen bond, as the greatest effect, was expected.

Generally, the hydrophobicity is favorable for the bioaccumulation, or the bioconcentration, of organic compounds.⁴² Therefore, a low value of the 1-octanol/water partition coefficient is required for new insecticides, to avoid the bioaccumulation. Our results of 1-octanol/water partition coefficients obtained in indirect experimental method can be used as an approximation to the direct experimental method of dilute samples of IL in saturated binary phases. However, our results assume the solubility of IL in the saturated solution of water in 1-octanol and reversely, contrary to the information published recently by Ropel et al.⁴³ For simple imidazole molecules our results were similar to the literature data.⁴⁴

Acknowledgment. Funding for this research was provided by the Polish State Committee (KBN) for Scientific Research (under Grant No. 3 T09B 004 27).

Supporting Information Available: General remarks regarding nuclear magnetic resonance (GRS 1), Fourier transform infrared spectroscopy (GRS 2), and mass spectroscopy (GRS 3). Tables describing specific details in regard to the properties of the 1-octanol/water system. Figures showing various equilibria diagrams. (All PDF.) This material is available free of charge via the Internet at <http://pubs.acs.org>.

References and Notes

- Ogihara, W.; Sun, J.; Forsyth, M.; MacFarlane, D. R.; Yoshizawa, M.; Ohno, H. *Electrochim. Acta* **2004**, *49*, 1797–1801.
- Lewandowski, A.; Stępiński, I. *Phys. Chem. Chem. Phys.* **2003**, *5*, 4215–4218.
- Visser, E.; Swatoski, R. P.; Reichert, W. M.; Griffin, S. T.; Rogers, R. D. *Ind. Eng. Chem. Res.* **2000**, *39*, 3596–3604.
- Wasserscheid, P.; Keim, W. *Angew. Chem.* **2000**, *112*, 3926–3945; *Angew. Chem., Int. Ed.* **2000**, *39*, 3773–3789.
- Wilkes, J. S. *J. Mol. Catal. A: Chem.* **2004**, *214*, 11–17.
- Visser, A. E.; Rogers, R. D. *J. Solid State Chem.* **2003**, *171*, 109–113.
- Blanchard, L. A.; Gu, Z.; Brennecke, J. F. *J. Phys. Chem. B* **2001**, *105*, 2437–2444.
- Domańska, U.; Bogel-Lukasik, E.; Bogel-Lukasik, R. *Chem.–Eur. J.* **2003**, *9*, 3033–3041.
- Domańska, U.; Bogel-Lukasik, E.; Bogel-Lukasik, R. *J. Phys. Chem. B* **2003**, *107*, 1858–1863.
- Domańska, U.; Marciniak, A.; Bogel-Lukasik, R. *Ionic Liquids III*; ACS Symposium Series 901–902; American Chemical Society: Washington, DC, 2005.
- Domańska, U.; Marciniak, A. *J. Phys. Chem. B* **2004**, *108*, 2376–2382.
- Lygo, B.; Crosby, J.; Peterson, J. A. *Tetrahedron Lett.* **1999**, *40*, 1385–1388.
- Ooi, T.; Kameda, M.; Maruoka, K. *J. Am. Chem. Soc.* **1999**, *121*, 6519–6520.
- Kim, D. Y.; Huh, S. C.; Kim, S. M. *Tetrahedron Lett.* **2001**, *42*, 6299–6301.
- Chinchilla, R.; Mazon, P.; Najera, C. *Tetrahedron: Asymmetry* **2002**, *13*, 927–931.
- Morrow, T. I.; Maginn, E. *J. Fluid Phase Equilib.* **2004**, *217*, 97–104.
- Abbott, A. P.; Capper, G.; Davies, D. L.; Rasheed, R. K. *Chem.–Eur. J.* **2004**, *10*, 3769–3774.
- Abbott, A. P.; Capper, G.; Davies, D. L.; Rasheed, R. K.; Tambyrajah, V. *Green Chem.* **2002**, *4*, 24–26.
- Eike, D. M.; Brennecke, J. F.; Maginn, E. *J. Green Chem.* **2003**, *5*, 323–328.
- Pernak, J.; Chwała, P.; Syguda, A. *Pol. J. Chem.* **2004**, *78*, 539–546.
- Crosthwaite, J. M.; Aki, S. N. V. K.; Maginn, E. J.; Brennecke, J. F. *J. Phys. Chem. B* **2004**, *108*, 5113–5119.

- (22) Crosthwaite, J. M.; Aki, S. N. V. K.; Maginn, E. J.; Brennecke, J. F. *Fluid Phase Equilib.* **2005**, 228–229, 303–309.
- (23) Anthony, J. L.; Maginn, E. J.; Brennecke, J. F. *J. Phys. Chem. B* **2001**, 105, 10942–10949.
- (24) Scurto, A. M.; Aki, S. N. V. K.; Brennecke, J. F. *J. Am. Chem. Soc.* **2002**, 124, 10276–10277.
- (25) Cadena, C.; Anthony, J. L.; Shah, J. K.; Morrow, T. I.; Brennecke, J. F.; Maginn, E. J. *J. Am. Chem. Soc.* **2004**, 126, 5300–5308.
- (26) Anthony, J. L.; Maginn, E. J.; Brennecke, J. F. *J. Phys. Chem. B* **2002**, 106, 7315–7320.
- (27) Kazarian, S. G.; Briscoe, B. J.; Welton, T. *J. Chem. Soc., Chem. Commun.* **2000**, 2047–2048.
- (28) Guadagno, T.; Kazarian, S. G. *J. Phys. Chem. B* **2004**, 108, 13995–13999.
- (29) Baker, S. N.; Baker, G. A.; Kane, M. A.; Bright, F. V. *J. Phys. Chem. B* **2001**, 105, 9663–9668.
- (30) Cammarata, L.; Kazarian, S. G.; Salter, P. A.; Welton, T. *Phys. Chem. Chem. Phys.* **2001**, 3, 5192–5200.
- (31) Huddleston, J. G.; Willaner, H. D.; Swatoski, R. P.; Visser, A. E.; Rogers, R. D. *Chem. Commun.* **1998**, 1765–1766.
- (32) Abbott, A. P.; Capper, G.; Raymond, K. R.; Tambyrajah, V. *Chem. Commun.* **2003**, 70–71.
- (33) Domańska, U. *Fluid Phase Equilib.* **1986**, 26, 201–220.
- (34) Nagata, I. *Fluid Phase Equilib.* **1985**, 19, 153–174.
- (35) Nagata, I.; Nalamiya, Y.; Katoh, K.; Kayabu, J. *Thermochim. Acta* **1981**, 45, 153–165.
- (36) Barton, A. F. M. *CRC Handbook of Solubility Parameters*; CRC Press: Boca Raton, FL, 1985; p 64.
- (37) Values calculated according to the van't Hoff relation. (From Nagata, I. *Thermochim. Acta* **1986**, 107, 199–217.)
- (38) Nath, A.; Bender, E. *Fluid Phase Equilib.* **1981**, 7, 289–293.
- (39) Dallas, A. J.; Carr, P. W. *J. Chem. Soc., Perkin Trans.* **1992**, 2, 2155–2160.
- (40) Butcher, J. A. IRG Document No. IRG/WP/3328, International Research Group on Wood Preservation, Stockholm, Sweden, 1985.
- (41) Palczewska-Tulińska, M. D.; Wyrzykowska-Stankiewicz, A. M.; Szafranski, J.; Choliński, *Solid And Liquid Heat Capacity Data Collection, Part 2: C6–C33*, DECHEMA e. V. 4: Germany, 1997; pp 1610, 1628, 1638, 1648, 1658.
- (42) Sandler, S. I.; Orbey, H. *Fluid Phase Equilib.* **1993**, 82, 63–69.
- (43) Ropel, L.; Belvéze, L. S.; Aki, M. S. N. V. K.; Stadtherr, M. A.; Brennecke, J. F. *Green Chem.* **2005**, 7, 83–90.
- (44) Domańska, U.; Kozłowska, M. K.; Rogalski, M. *J. Chem. Eng. Data* **2002**, 47, 456–466.